Modulation of Aldose Reductase Activity by Aldose Hemiacetals

Francesco Balestri[1], Mario Cappiello[1,2], Roberta Moschini[1,2], Rossella Rotondo[1], Marco Abate[3], Antonella Del-Corso[1,2] and Umberto Mura[1,2].

[1]University of Pisa, Department of Biology, Biochemistry Unit, via San Zeno, 51, Pisa, 56127 Italy;

[2]Interdepartmental Research Center Nutrafood ‘‘Nutraceuticals and Food for Health’’, University of Pisa, Pisa, Italy

[3]University of Pisa, Department of Mathematics, via Buonarroti, 2, Pisa, 56127 Italy;

Corresponding author: Antonella Del-Corso, Department of Biology, Biochemistry Unit, Via S. Zeno,51, Pisa, Italy; Tel: 39(050) 2211454; Fax: 39(050) 2211460; E-mail: antonella.delcorso@unipi.it

The abbreviations used are: AR, aldose reductase; ARIs, aldose reductase inhibitors; HNE, *trans*-4-hydroxy-2,3-nonenal; ARDIs, aldose reductase differential inhibitors; 2-ME, 2-mercaptoethanol; DTT, D,L-dithiothreitol; *h*AR, human placental recombinant aldose reductase; *b*AR, bovine lens aldose reductase; GAL, D,L-glyceraldehyde; SB, 10 mM sodium phosphate buffer pH 7.0;

ABSTRACT

Background: Glucose is considered as one of the main sources of cell damage related to aldose reductase (AR) action in hyperglycemic conditions and a worldwide effort is posed in searching for specific inhibitors of the enzyme. This AR substrate has often been reported as generating non hyperbolic kinetics, mimicking a negative cooperative behavior. This feature was explained by the simultaneous action of two enzyme forms acting on the same substrate.

Methods: The reduction of different aldoses and other classical AR substrates was studied using pure preparations of bovine lens and human recombinant AR.

Results: The apparent cooperative behavior of AR acting on glucose and other hexoses and pentoses, but not on tethroses, glyceraldehyde, 4-hydroxynonenal and 4-nitrobenzaldehyde, is generated by a partial nonclassical competitive inhibition exerted by the aldose hemiacetal on the reduction of the free aldehyde. A kinetic model is proposed and kinetic parameters are determined for the reduction of L-idose.

Conclusions: Due to the unavoidable presence of the hemiacetal, glucose reduction by AR occurs under different conditions with respect to other relevant AR-substrates, such as alkanals and alkenals, coming from membrane lipid peroxidation. This may have implications in searching for AR inhibitors. The emerging kinetic parameters for the aldoses free aldehyde indicate the remarkable ability of the enzyme to interact and reduce highly hydrophilic and bulky substrates.

General Significance: The discovery of aldose reductase modulation by hemiacetals offers a new perspective in searching for aldose reductase inhibitors to be developed as drugs counteracting the onset of diabetic complications.

Key words: aldose reductase; partial inhibition; glucose; hemiacetal; L-idose; diabetes.

1 INTRODUCTION

The NADPH-dependent reduction of D-glucose catalyzed by aldose reductase (E.C.1.1.1.21) (AR) is considered as one of the phenomena leading to the onset of long term diabetic complications [as review see: 1, 2]. In fact, the reduction of the sugar, which occurs mainly in hyperglycemic conditions, is associated with a number of deleterious events. Stressful and damaging cell conditions are caused by a number of factors: the osmotic imbalance due to sorbitol accumulation [3], the loss of reducing, and thus, antioxidant power associated to NADPH oxidation [4] and the induction of more favorable conditions for protein glycation [5]. This led a strong impulse in the search for molecules able to efficiently inhibit the enzyme (aldose reductase inhibitors, ARIs) with

the aim to develop active drugs to antagonize the onset of diabetic complications. Several powerful ARIs have been proposed on the basis of their in vitro action, however the promotion of those molecules for effective drugs was not very successful; to date Japan and India are the only countries where an Epalrestat-based drug is distributed. This is likely due to the ability of AR to act on toxic hydrophobic aldehydes, derived from lipid peroxidation processes, such as *trans*-4-hydroxy-2,3-nonenal (HNE) [6, 7], whose reduction attenuates their cytotoxicity. Thus, AR inhibition would no longer appear to be a useful approach in favoring cell health [8-10]. Nevertheless, several experimental evidences suggest an anti-inflammatory action of ARIs [11]; this on the basis of the ability of AR to reduce the adduct between HNE and glutathione, generating a pro-inflammatory signal [6, 7, 12-14]. More recently a new approach to control AR activity by differential inhibition was proposed [15]. In this case, the inhibitors (AR differential inhibitors, ARDIs) should be able to inhibit AR while acting on glucose, but not on molecules such as HNE, whose breakdown is part of the detoxifying action exerted by AR.

The reaction rate of AR as a function of substrate concentration has been reported to display, in some instances, a negative cooperative type of behavior [16-26]. As AR is unequivocally a monomeric enzyme, the observed negative cooperativity was associated to the presence, in the enzyme preparations, of two enzyme forms, which were often referred to as the "unactivated" and the "activated" enzyme and displayed different kinetic properties, including a different susceptibility to inhibition by ARIs and by substrates [16, 18, 21, 25, 26]. Indeed, a fascinating and intriguing mechanistic explanation has been proposed to justify, despite the presence of the two enzyme forms, the hyperbolic behavior occasionally observed with glyceraldehyde or glycol aldehyde [27]. None of the above considerations are easy to rationalize, since in the literature it is difficult to find a common established procedure for enzyme preparation and manipulation in order to define which form of AR is present.

Although it has been reported that AR from the human psoas muscle could be modified by treatment with pyridoxal phosphate followed by $NaBH_4$ treatment [28], the only reversible covalent modification assessed for the enzyme to date has been the thiolation of Cys298. This is induced by different thiol compounds, including 2-mercaptoethanol (2-ME), in oxidative conditions, with consequent possible intramolecular trans-thiolation arrangements [29-34]. In addition, a S-glutathionyl-modified AR, a relatively stable enzyme form, not susceptible to Sorbinil inhibition and still sensitive to dithiothreitol (DTT) reduction, has been generated *in situ* in intact bovine lenses undergoing oxidative stress [35, 36]. On this basis, the occurrence of an apparent negative cooperative behavior that has been reported for the reduction of different substrates could be associated with the presence in pure enzyme preparations of enzyme forms with an altered cysteine

redox status, deriving from inappropriate thiol-reducing conditions (i.e. the use of 2-ME) adopted during enzyme purification and storage [29].

In this study, using pure enzyme preparations of human placental recombinant AR (*h*AR) and of AR isolated from bovine lens (*b*AR), which behave as Michaelis enzymes with glyceraldehyde as substrate, is shown that an apparent negative cooperativity action for glucose still occurs. We present evidence for a partial inhibitory action of the hemiacetal form of aldoses on the AR activity. A kinetic model is proposed to explain the apparent negative cooperative behavior observed for glucose and more generally for aldoses that are able to produce cyclic hemiacetal structures.

2 Materials and Methods

2.1 Materials

L-glucose, L-idose, L-sorbose and L-threose were from Carbosynth. D-fructose, D-glucose, D,L-glyceraldehyde (GAL), NADPH, 4-nitrobenzaldehyde and D-ribose were from Sigma Aldrich. DTT was from Inalco. HNE was prepared as described [37]. All other chemicals were of reagent grade.

2.2 Assay of aldose reductase.

The activity of AR was determined at 37°C following the decrease in absorbance at 340 nm due to NADPH oxidation (ε_{340} = 6.22 $mM^{-1}\cdot cm^{-1}$). The standard assay mixture contained 0.25 M sodium phosphate buffer pH 6.8, 0.18 mM NADPH, 2.4 M ammonium sulfate, 0.5 mM EDTA and 4.7 mM GAL. One unit of enzyme activity is the amount that catalyzes the conversion of 1 μmol of substrate/min in the above assay conditions. The above assay conditions were adopted also when D-glucose or L-idose were used as substrates instead of GAL.

2.3 Purification of human recombinant and bovine lens AR.

The *h*AR was expressed as previously described [38]. Both *b*AR and *h*AR were purified following essentially the same procedure [39]. The purity of enzyme preparations was assessed by SDS-PAGE [40] and gels were stained with silver nitrate [41]; both enzyme preparations showed a unique band corresponding to a molecular weight of approximately 34 KDa. The specific activity of purified *b*AR and *h*AR was 1.2 and 5.3 U/mg, respectively. The purified *b*AR and *h*AR were stored at -80 °C in 10 mM sodium phosphate buffer pH 7.0 (SB) containing 2 mM DTT alone or with 30% (w/v) glycerol, respectively. Both enzymes were extensively dialyzed against SB before use.

2.4 Other methods.

Protein concentration was determined according to Bradford [42].

"GraphPad 6.0" was used for statistical analysis and for determination, by hyperbolic nonlinear regression analysis, of kinetic parameters. The analysis was performed for different substrates on two sets of data, referring to "low" and "high" substrate concentration ranges, which are specified for the different aldoses. Double reciprocal plots of kinetic measurements are adopted only for presentation of experimental data. The straight lines in these plots were drawn on the basis of the kinetic parameters (i.e. intercepts on the ordinate and abscissa axes) derived from nonlinear regression analysis of experimental data. To determine the fitting curve for nonrectangular hyperbolic functions (i.e. $y = (a + bx)/(c + dx)$), as is the case of data reported in Fig. 6 and Fig. 7, inset, a least squares method was used. The optimization of the parameters for determining the best fit was performed with the Levenberg-Marquardt algorithm; the computations were performed with the symbolic mathematical computational software "Mathematica".

The concentrations of the free aldehyde form of D-glucose and L-idose were calculated from the following percentage of open chain: 1.28 x 10^{-3} % and 87.70 x 10^{-3} %, respectively [43].

3 RESULTS

3.1 Kinetic analysis of aldoses reduction by AR.

Rate measurements of glucose reduction catalyzed by *b*AR and *h*AR, performed using a wider range of substrate concentration than previously adopted [38], are reported in Fig. 1. The resulting behavior appears consistent with a complex kinetic mechanism mimicking an apparent negative cooperative model of action. Through nonlinear regression analysis, two different values for apparent K_M (74.9 ± 3.2 and 8.5 ± 2.9 mM for *b*AR and 204.6 ± 20.4 and 24.1 ± 7.6 mM for *h*AR) and k_{cat} (0.84 ± 0.02 and 0.14 ± 0.03 s^{-1} for *b*AR and 1.84 ± 0.09 and 0.28 ± 0.13 $s^{-1}$for *h*AR) were determined for the high and low range of glucose concentrations, respectively. The high and low range of glucose concentrations refer to: for *h*AR 12-400 mM and 5.5-10 mM, respectively; for *b*AR 6.5-100 mM and 3-6 mM, respectively.

In this study, to avoid the generation of different oxidized enzyme forms, pure enzyme preparations freshly dialyzed against SB to remove 2 mM DTT present during storage at –80°C, were used. In addition, pure enzyme preparations still containing DTT (0.1 mM final concentration in the assay mixture) generate, using glucose as substrate, a biphasic curve as those of Fig. 1 (data not shown). On the other hand, a linear behavior in double reciprocal plots for GAL, D-erythrose, L-threose, HNE, and 4-nitrobenzaldehyde was observed (Fig. 2). A unique straight line could be drawn for

these substrates when the nonlinear regression analysis was performed on two sets of rate measurements, at high and low substrate concentrations (data not shown).
In order to assess whether the biphasic kinetics is a particular feature of glucose reduction, different long chain aldoses (more than 4 carbon atoms) were tested as substrates for AR in a wide range of substrate concentrations. Double reciprocal plots of the *hAR*-catalyzed reduction of D-Galactose, L-idose, D-Ribose and D-xylose are reported in Fig. 3. As shown, irrespectively of their apparent effectiveness as substrates, all the tested molecules display a biphasic behavior, since for all of them it is possible to evaluate limiting values of apparent kinetic parameters (see Section 2.4) for the high and low substrate concentration ranges (data not shown).

3.2 A kinetic model for aldose reduction by AR

In order to verify the potential of the multiple interaction of aldose hemiacetal and free aldehyde components on AR as causative of the apparent negative behavior displayed by glucose and other aldoses undergoing reduction, different partial inhibition pathways, namely, the nonclassical competitive, the mixed noncompetitive and the uncompetitive, were considered (Fig. 4 Panels A, B and C, respectively). No specific restrictions are imposed on the values of the kinetic constants k_{+2} and k_{+4} except that they should not to be significantly different. Here is considered that the aldose free aldehyde form is the only one susceptible to reduction [44] and that the ternary complex between AR, the free aldehyde and the aldose hemiacetal is still able to generate products. It is worth noting that a possible competition between the aldose hemiacetal and the free aldehyde as substrates for the enzyme does not explain the apparent negative cooperative behavior observed for aldoses reduction [45] (see also Appendix-Sect.V). On the other hand, there is evidence that AR is unable to catalyze the ring opening of glucose hemiacetal [46].
By considering the interaction steps of the substrate (A) as in a steady state condition and those involving the hemiacetal (C) at the equilibrium, the above kinetic models were analyzed.
The nonclassical competitive model (Fig. 4 A) proposes that the hemiacetal form (*C*) can specifically interact with the free enzyme, allowing the free aldehyde substrate (*A*) to still enter into the catalytic site and undergo reduction.
The general rate equation for this model can be written as:

$$v_0 = \frac{d[P]}{dt} = k_{+2}[EA] + k_{+4}[ECA] \quad (1)$$

By applying equilibrium conditions for all the equilibrium steps [47], or the steady state condition for *EA* and *ECA* and considering the *EC* complex at the equilibrium, the following kinetic equation can be formulated for the transformation of the substrate (see Appendix-Sect.I):

$$v_0 = \frac{E_T \frac{k_{+2}\, K'_m K_i + k_{+4} K_m [C]}{K_m [C] + K'_m K_{EC}} [A]}{\frac{K_m\, K'_m (K_i + [C])}{K'_m K_i + K_m [C]} + [A]} \qquad (2)$$

where $K_m = (k_{+2} + k_{-1})/k_{+1}$ and $K'_m = (k_{+4} + k_{-3})/k_{+3}$ represent the Michaelis constants for the free aldehyde of *E* and *EC*, respectively, while K_i represents the dissociation constant of *EC*. Equation 2 enables the effect exerted on the reaction rate by either the hemiacetal or the sugar free aldehyde to be predicted. When one of these two terms is kept constant, as shown, for instance, for *C* in the Eq.2, the dependence of the reaction rate on the other one is hyperbolic.

In order to interpret the biphasic behavior of glucose and, more generally, of aldose reduction (Fig. l and Fig. 3), Eq.2 was rewritten by expressing $[C]$ and $[A]$ in terms of total glucose concentration $[G]$. Thus, given that:

$[C] + [A] = [G]$ and $\frac{[C]}{[A]} = R$

it follows that:

$[A] = \frac{[G]}{R+1}$ and $[C] = \frac{R[G]}{R+1}$

The substitution of these terms in Eq.1 and simple algebra steps gives Eq.2 (see Appendix-Sect.I):

$$v_0 = \frac{E_T \{k_{+2}\, K'_m\, K'_i (R+1)[G] + k_{+4} K_m R [G]^2\}}{K_m K'_m K_i (R+1)^2 + K'_m (K_m R + K_i)(R+1)[G] + K_m R [G]^2} \ldots (3)$$

Equation 3 describes a complex kinetic behavior that fits the data of the reaction rates of the AR-catalyzed aldose reduction as a function of the nominal aldose concentration (Figs. 1 and 3) In fact, using the kinetic parameters determined in the present study for L-idose reduction (see below) and taking into account the free aldehyde present in L-idose solutions [43], a computer-assisted simulation enables calculated curves for L-idose to fit with kinetic measurements (Fig. 5, curve 1).

When considering the mixed type of inhibition (Fig. 4 B), starting from the general kinetic equation:

$v_0 = \frac{d[P]}{dt} = k_{+2}[EA] + k_{+4}[EAC]$ (4)

a kinetic equation as a function of both hemiacetal and free aldehyde concentration (Eq.5), can be obtained (see Appendix-Sect.II):

$$v_0 = \frac{\frac{E_T \left(k_{+2} K'_m\, K'_i\, K_i + k_{+4} \left(K_m\, K'_i + K'_m K_i \right) [C] \right)}{K'_m\, K'_i\, K_i + \left(K_m\, K'_i + K'_m K_i \right) [C]} [A]}{\frac{K_m\, K'_m K'_i (K_i + [C])}{K'_m\, K_i K'_i + \left(K_m\, K'_i + K'_m K_i \right) [C]} + [A]} \qquad (5)$$

When expressed in terms of nominal aldose concentration (i.e. [G]) Eq.5 becomes:

$$v_0 = \frac{E_T\{k_{+2}\, K'_m K_i\, K'_i(R+1)[G] + k_{+4}R(K_m\, K'_i + K'_m K_i)[G]^2\}}{K_m\, K'_m K_i\, K'_i(R+1)^2 + K'_m\, K'_i(R+1)(K_m R + K_i)[G] + R(K_m\, K'_i + K'_m K_i)[G]^2} \quad (6)$$

Thus, also this mechanism of inhibition may explain the downwards curvature observed in double reciprocal plots for AR catalyzed reduction of the aldoses. This occurs, however, only when a more favorable binding of the hemiacetal to *E*, with respect to *EA*, occurs. In fact, as shown in Fig. 5, a shift from an upward curvature to a downward curvature (curves 2 to 5) occurs when K'_i/K_i was increased from 0.5 to 50. As shown, at the highest K'_i/K_i ratio the curve is essentially superimposable to curve 1 coming from Eq.3.

Different is the case of an exclusive interaction of *C* with the *EA* complex (Fig. 4 C). For this partial uncompetitive model of action in which, even not shown, the *EC* complex generated from the catalytic step promptly dissociates, the emerging kinetic equations in terms of both hemiacetal and free aldehyde concentration (Eq.7) and in terms of total aldose concentration (Eq.8) resulted:

$$v_0 = \frac{\frac{E_T(k_{+2}\, K'_i + k_{+4}[C])}{(K'_i + [C])}[A]}{\frac{K_m\, K'_i}{K'_i + [C]} + [A]} \quad (7)$$

$$v_0 = \frac{E_T\{k_{+2}\, K'_i(R+1)[G] + k_{+4}R[G]^2\}}{K_m\, K'_i(R+1)^2 + K'_i(R+1)[G] + R[G]^2} \quad (8)$$

Equation 8 would appear in the double reciprocal plots with an upward curvature, as occurs for apparent positive cooperativity or substrate inhibition models (data not shown). This would not fit with the downward curves observed for long chain aldoses (Figs. 1 and 3).

3.3 Interaction of hemiacetals with AR.

The potential of a partial inhibitory action exerted by the hemiacetal form on the aldose reduction was verified by evaluating the effect exerted by D-glucose on the reduction of L-idose. This was achieved by measuring NADPH oxidation using as a substrate 0.4 mM L-idose (a concentration which accounts for 0.35 µM of L-idose free aldehyde) with different concentrations of D-glucose in a sufficiently low range (up to 4 mM, accounting for 0.05 µM of the free aldehyde) so as not to impact on the overall AR-dependent oxidation of the cofactor (Fig. 6). In these conditions there was an inhibitory action of D-glucose on L-idose reduction of approximately 10 % at the highest tested concentration. When L-glucose, which is not recognized as a substrate for AR (no activity could be detected in standard assay conditions with 30 mM of the sugar), was used instead of D-glucose as a source of hemiacetal, a maximal inhibition of 17 % was evaluated. The same figure shows that

hemiketals, such as D-fructose and L-sorbose, were ineffective in modulating the AR-dependent reduction of L-idose. Finally, we found that L-glucose inhibits the reduction of D-ribose.

In order to explore the model of partial inhibition exerted by hemiacetals on the AR-catalyzed L-idose reduction, a set of assay mixtures was assembled to evaluate the dependence of the reaction rate on the concentration of L-idose, with different fixed levels of hemiacetal. This was achieved by complementing with L-glucose the difference in hemiacetal concentration occurring at different L-idose concentrations. When reported in double reciprocal plots, the reaction rates measured at different substrate concentrations appear as straight lines that nearly converge on the ordinate axis, with slopes that increase with the increase in L-glucose concentration (Fig. 7). This result is expected for all the considered inhibition models on the basis of Eqs.2, 5 and 7.

Having made no assumptions on the relative values of k_{+2} and k_{+4} (Fig. 4), except for not significant differences among them, V_{max}^{app} will change for all the models from $k_{+2}E_T$ to $k_{+4}E_T$ with the increase in [*C*] through a hyperbolic function of general form $y = (a+bx)/(c+dx)$ (see Appendix-Sect.IV). In contrast, the K_M^{app} values, through a similar hyperbolic function, will increase with the increase in [*C*] in the case of nonclassical competitive interaction, while they will decrease in the case of uncompetitive interaction. In the case of the mixed type of inhibition K_M^{app} values versus [C] concentration will either increase or decrease, through a hyperbolic function, from K_m towards the limit value of $K_m\ K_i'$ or $K_m'\ K_i$ depending on the relative values of K_i and K_i'.

The secondary plot of apparent K_M values (Fig. 7, inset), derived from nonlinear regression analysis of data shown in Fig. 7, enables the relative affinity of the aldose free aldehyde for the free AR to be assessed, as well as for the hemiacetal-bound enzyme (see Appendix, Sect.I and Sect.IV). As it is impossible to measure the enzyme activity in the absence of the hemiacetal, the limit apparent K_M values at zero (K_m) and at saturating (K_m') hemiacetal concentrations were determined by analyzing the secondary plot curve (Fig. 7, inset) by a nonlinear fitting method using a general equation $y = (a+bx)/(c+dx)$ (see Section 2.4). Thus, we were able to estimate values of 1.0 ± 0.6 μM and 3.4 ± 0.5 μM for K_m and K_m', respectively. Similarly, the apparent V_{max} values (derived from nonlinear regression of data of Fig. 7) were analyzed by a nonlinear fitting method (Fig. 7, inset). A tendency to increase of V_{max} from 0.014 ± 0.005 mM min^{-1} to 0.026 ± 0.002 mM min^{-1} was evaluated.

4 DISCUSSION

The biphasic kinetic behavior occasionally reported for the reduction of different substrates, including D-glucose, by AR and associated with the possible presence of two enzyme forms [16, 18, 21, 25, 26], was also observed in the present work, in which all precautions were taken to

prevent an oxidative modification of the purified *b*AR and *h*AR. Thus, DTT, as thiol reducing agent, and EDTA (also present in the AR assay mixture) never left AR during extraction and purification (except, necessarily, for the time needed to perform the affinity chromatography step). In addition, the use of 2-ME was completely avoided. In fact, 2-ME, so often used as a preservative for reduced thiols, has been found to be a very efficient trigger of AR oxidative modification, when often uncontrolled factors (storage time and conditions, temperature, traces of transition metal ions, disulfides) induce its full or partial oxidation [29]. Paradigmatic is the reported evidence of a purified AR preparation that was isolated from human psoas muscle in the presence of 5 mM 2ME and which resulted to be inactivated (we would say re-converted to its native form) by DTT, but not by 2ME [48]. Finally, the ionic strength stress, as occurs during ammonium sulfate fractionation, which forces the release from AR of the bound pyridine cofactor [39], especially during earlier purification steps, was avoided in order to preserve AR in its native state [30, 49].

With the above-mentioned precautions, the final highly-purified preparations of both *b*AR (data not shown) and *h*AR behave, as expected, as monomeric catalysts characterized by simple hyperbolic kinetics when D-erythrose, L-threose, GAL, HNE and 4-nitrobenzaldehyde were used as substrates in a range of concentrations in which substrate inhibition phenomena can be ruled out (Fig. 2). The linearity observed with GAL, L-threose or D-erythrose by itself does not rule out the presence of two enzyme forms. In fact an inhibitory adduct between the enol form of the substrate and the oxidized pyridine cofactor, which would mask the biphasic behavior expected as a consequence of the presence of two enzyme forms, can be generated [27]. However, the linearity observed with HNE, which is more susceptible as a target by nucleophilic attack at the C3 than as nucleophile on the pyridine ring of $NADP^+$, and with 4-nitrobenzaldehyde, a molecule that is unable to enolize and therefore is not able to generate the inhibitory adduct, confirms the absence of different forms of AR in the used enzyme preparations.

The results obtained with D-glucose (Fig. 1) enable two couples of kinetic parameters to be estimated, namely K_M and k_{cat}, measured at high and at low substrate concentrations. For each kinetic parameter an approximately 10 fold difference was observed between the high and low range of substrate concentration. These results explain the wide range of kinetic parameters values reported to date for glucose in the literature [30, 50-54]. However, having ruled out the presence of two enzymatic forms concurring to the reduction of glucose, as is the case of the present study, interpreting the above apparent kinetic parameters becomes conceptually difficult.

Thus, the observed apparent negative cooperative reduction of D-glucose was associated with the particular features of this substrate, rather than with the combined action of two different enzyme forms. We found that this effect was the result of a partial inhibitory action exerted by the glucose

hemiacetal on the reduction of glucose free aldehyde. This biphasic behavior is not unique for D-glucose, but is a general feature of the long chain aldoses that generate cyclic hemiacetals. In fact, the reduction processes of L-idose, D-galactose, D-ribose and D-xylose catalyzed by *h*AR, all display apparent negative cooperative features (Fig. 3). It thus follows that the proposed interaction of cyclic hemiacetal with the enzyme is not a special feature of glucose hemiacetal, but applies to the hemiacetal structures of the tested 5 and 6 carbon atom aldoses, which all modulate the reduction of their respective open aldehyde forms.

We found evidence of the interaction between AR and hemiacetals by evaluating the effect of glucose on L-idose reduction. L-idose was recently proposed as the best AR substrate able to mimic glucose [38]. This aldose is structurally very closely related to D-glucose, from which it differs only in the stereo chemical configuration of the C_5 carbon atom. The two aldoses, however, significantly differ in terms of the content of the free aldehyde, with L-idose, of the aldoses, having one of the highest contents of the free aldehyde form in aqueous solution (60 to 80 fold higher than glucose) [43]. Given that glucose free aldehyde represents approximately only 1.28×10^{-3} % of total glucose, we verified the effect of the hemiacetal form of glucose on L-idose reduction by avoiding the interference exerted by the reduction of glucose itself. Using 0.4 mM L-idose as substrate, a modest inhibition, progressively increasing up to approximately 10% of the initial enzyme activity, was observed when D-glucose was increased in the assay mixture from zero to 4 mM (Fig. 6). Higher D-glucose concentrations could not be tested because of the contribution of glucose reduction to the overall AR activity. L-glucose is a very poor substrate for the enzyme. It is thus an ideal tool to evaluate the hemiacetal inhibition, since no contribution is expected in the activity measurements for at least up to 30 mM of the sugar. When L-glucose, rather than D-glucose, was used as a source of hemiacetal a progressive increase of the inhibitory effect on L-idose reduction was observed up to approximately 17%. The observed inhibitory effect may be underestimated, since it is impossible to measure the enzyme activity on long chain aldoses in the absence of the hemiacetal form. In fact, when the data related to the inhibition of L-glucose on L-idose reduction were analyzed by a nonlinear fitting program (see Section 2.4), the values of the rate extrapolated to a zero hemiacetal concentration (2.52×10^{-3} mM min^{-1}) and to an infinitive hemiacetal concentration (1.86×10^{-3} mM min^{-1}) revealed an inhibitory effect of approximately 26%.

This result, together with the biphasic effect observed for several long chain aldoses (Fig. 3), suggests an apparent broad specificity of the enzyme for cyclic hemiacetals of different aldoses. The interaction, however, displays some specificity, since hemiketal structures, such as those generated by D-fructose and L-sorbose, did not affect the enzyme's activity (Fig. 6).

The case of L-threose and D-erythrose is also worth noting; the reduction of these aldoses did not appear to be affected by their hemiacetal form. Either the furanosidic hemiacetal form, the only one compatible with 4 carbon atom aldoses, is unable to interact with the enzyme, or the hemiacetal/free aldehyde ratio is too low to generate a biphasic response. It is also possible that the molecular size and/or the hindrance of L-threose and D-erythrose enable the free aldehyde of these sugars to escape the inhibitory action of furanosidic hemiacetals. However, the fact that the reduction of these sugars, as also occurs for GAL, was not affected by L-glucose (data not shown), suggests that they are not affected by the perturbation of the AR active site induced by hemiacetals.

On the basis of indications emerging from Eqs. 2, 5 and 7, it was possible to have insight in the mechanism of action of the hemiacetal on the free aldehyde reduction. The analysis of kinetic parameters measured for L-idose at different fixed levels of hemiacetal (Fig. 7) indicates that some effect on the catalytic step of aldehyde reduction may occur. In fact, an increase in apparent k_{cat}, from 1.24 ± 0.48 s^{-1} to 2.32 ± 0.19 s^{-1} was observed (Fig.7, inset). More evident is the increase in apparent K_M up to three fold, from approximately 1 µM (K_m) to 3.4 µM (K'_m) , with the increase in hemiacetal concentration. The absolute values of these kinetic parameters may be debatable, because of the resulting rather high error. However, because of the high confidence limits of the data fitting, the trend of the parameters with the increase in hemiacetal concentration is unequivocal. The emerging values for the kinetic parameters related to the hemiacetal-bound AR (i.e. k_{+4} and K'_m) are essentially the same as those previously measured for L-idose reduction analyzed in the high range of substrate concentrations [38]. Indeed, using the above kinetic parameters measured for L-idose, a biphasic double reciprocal plot, generated by a computer-assisted simulation of Eq.2, was able to fit experimental results of Fig. 3 A, by imposing a value of K_i of 2.5 x 10^{-4} M (Fig. 5). In principle, a partial uncompetitive inhibition model can also generate an apparent cooperative behavior (see Appendix, Sect.III). However, this inhibition model can be ruled out, since the biphasic curves in the double reciprocal plot would appear with an upward curvature, as would happen with an apparent positive cooperativity or substrate inhibition. This is strengthened by the progressive increase of apparent K_M values of L-idose free aldehyde with the increase of hemiacetal concentration (Fig. 7, inset) which is incompatible with a uncompetitive inhibition model (Eq.7). As previously mentioned, our data are unable to discriminate between nonclassical competitive from mixed noncompetitive inhibition models. Thus the latter mechanism, which must be characterized in any event by a significant contribution of the competitive interaction (Fig. 5), cannot be ruled out.

In conclusion, our study would seem to indicate that a hydrophilic microenvironment, which is suitable to accomodate highly hydrophilic molecules with steric hindrance such as aldose hemiacetals, allows the enzyme modulation by one of its most important physiopathological substrates. It is difficult at the moment to envisage the physical placement of the hemiacetal on the enzyme. Nevertheless the flexibility and adaptability of the induced cavity region at the inhibitory site of AR [55, 56] may contribute to the hemiacetal binding.

While providing a plausible interpretation of the apparent negative cooperative behavior of the reduction of glucose and, in more general terms, of long chain aldoses by AR, the effect reported here of the hemiacetal ring on the enzyme activity strengthens the particular interaction of AR with aldoses compared to other non-sugar substrates. This increases the possibility of intervening on the enzyme by a differential inhibitory action, aimed at targeting the enzyme while working on glucose without, or only partially, affecting the reduction of hydrophobic cytotoxic aldehydes such as alkenals or alkanals (Del Corso et al., 2013). In any event, although modest in terms of absolute values, the partial inhibitory action of aldose hemiacetals is worth considering when planning kinetic studies of AR in which the enzyme is targeted for inhibition to develop drugs against the onset of diabetic complications. In fact the presence of an additional species (i.e. the hemiacetal), trafficking in or near by the AR active site, must be taken in consideration when performing in vitro studies for ARIs or ARDIs selection.

Finally, we found that the apparent low efficiency of AR towards glucose, which has so often led to the enzyme not to being considered tailored for hydrophilic molecules, is not only dramatically affected by the low level of the free aldehyde form present in solution, but also by the subtle inhibitory effect exerted by the hemiacetal ring of glucose itself.

APPENDIX

Kinetic models for aldose reduction by aldose reductase

Section I-*Partial inhibition for a nonclassical competitive model of action of aldose hemiacetal on the free aldehyde reduction.*

By considering the kinetic model of Fig. 4 A in which an exclusive interaction of *C* with the free enzyme occurs and starting from the general rate equation for the transformation of *A*:

$$v_0 = \frac{d[P]}{dt} = k_{+2}[EA] + k_{+4}[ECA] \qquad \text{(A.1)}$$

it follows:

$$K_i = \frac{[E][C]}{[EC]} \qquad \text{(A.2)}$$

$k_{+1}[E][A] = (k_{+2} + k_{-1})[EA]$ (A. 3)

$k_{+3}[EC][A] = (k_{+4} + k_{-3})[ECA]$ (A.4)

Different enzyme forms can be expressed in terms of [*EA*].

From Eq.(A.3):

$[E] = \frac{k_{+2}+k_{-1}}{k_{+1}[A]}[EA] = \frac{K_m}{[A]}[EA]$ (A.5)

From Eq.(A.2) and Eq.(A.5):

$[EC] = \frac{[E][C]}{K_i} = \frac{K_m[C]}{K_i[A]}[EA]$ (A.6)

From Eq. (A.4) and Eq. (A.6):

$[ECA] = \frac{k_{+3}[EC][A]}{k_{+4}+k_{-3}} = \frac{K_m[C]}{K'_m K_i}[EA]$ (A.7)

Taking into account the mass balance for the enzyme (Eq. (A.8))

$E_T = [E] + [EC] + [ECA] + [EA]$ (A.8)

and normalizing the reaction rate v_0 (Eq. (A.1)) for E_T:

$$\frac{v_0}{E_T} = \frac{k_{+2}[EA] + k_{+4}\frac{K_m[C]}{K_i K'_m}[EA]}{\frac{K_m}{[A]}[EA] + \frac{K_m[C]}{K_i[A]}[EA] + \frac{K_m[C]}{K_i K'_m}[EA] + [EA]}$$

Simplifying for [*EA*],

$$v_0 = \frac{E_T\left(k_{+2}+k_{+4}\frac{K_m[C]}{K_i K'_m}\right)}{\frac{K_m}{[A]}+\frac{K_m[C]}{K_i[A]}+\frac{K_m[C]}{K_i K'_m}+1}$$ (A.9)

Equation A.9 enables the effect exerted on the reaction rate by the concentration of both the hemiacetal ring and the sugar free aldehyde to be predicted. When one of these two parameters is kept constant, the dependence of the reaction rate on the other parameter is of hyperbolic type. At a fixed level of hemiacetal (i.e. [C] = constant), Eq. A.9 can be rewritten to appear in the usual form of a rectangular hyperbola:

$$v_0 = \frac{E_T\frac{k_{+2}K'_m K_i + k_{+4}K_m[C]}{K_m[C]+K'_m K_i}[A]}{\frac{K_m K'_m(K_i+[C])}{K'_m K_i + K_m[C]}+[A]}$$ (A.10, Eq. 2 in the text)

In order to express $[C]$ and $[A]$ in terms of total glucose concentration $[G]$, being:

$[C] + [A] = [G]$ (A.11)

and

$\frac{[C]}{[A]} = R$ (A.12)

it follows that:

$$[A] = \frac{[G]}{R+1} \quad \text{and} \quad [C] = \frac{R[G]}{R+1}$$

The substitution in Eq.(A.9) gives:

$$v_0 = \frac{E_T\{k_{+2}\, K'_m K_i\, (R+1) + k_{+4} K_m R[G]\}}{(R+1)\left(\frac{K_m\, K'_m K_i\, (R+1)}{[G]} + \frac{K_m\, K'_m K_i\, R}{K_i} + \frac{K_m\, K'_m K_i\, R[G]}{K'_m\, K_i (R+1)} + K_i\, K'_m\right)}$$

After simplification and simple algebra steps, the following results:

$$v_0 = \frac{E_T\{k_{+2}\, K'_m\, K'_i (R+1)[G] + k_{+4} K_m R[G]^2\}}{K_m K'_m K_i (R+1)^2 + K'_m (K_m R + K_i)(R+1)[G] + K_m R[G]^2} \qquad \text{(A.13, Eq.3 in the text)}$$

This equation describes the dependence of the reaction rate on the concentration of glucose and, imposing $K_m < K'_m$ it fits with an apparent negative cooperative behavior (i.e. downward curvature in the double reciprocal plots) as that observed for long chain aldoses (see text, Figs. 1 and 3).

Section II*-Partial inhibition for a mixed noncompetitive model of action of aldose hemiacetal on free aldehyde reduction.*

When the model of Fig. 4 B is analyzed considering *EC* and *EAC* at equilibrium, and *EA* and ECA in steady state conditions, the general rate equation for the transformation of *A:*

$$v_0 = \frac{d[P]}{dt} = k_{+2}[EA] + k_{+4}([EAC] + [ECA])$$

becomes :

$$v_0 = \frac{E_T\left\{k_{+2} + k_{+4}\left(\frac{[C]}{K'_i} + \frac{K_m[C]}{K'_m K_i}\right)\right\}}{\frac{K_m}{[A]} + \frac{K_m[C]}{K_i[A]} + \frac{K_m[C]}{K_i\, K'_m} + \frac{[C]}{K'_i} + 1} \qquad \text{(A.14)}$$

Equation (A.14) describes the dependence of the reaction rate of glucose reduction as a function of the aldose free aldehyde and aldose hemiacetal concentrations in the case of partial mixed noncompetitive type of inhibition. When one of these two terms is kept constant, v_0 versus the second one is described again by a rectangular hyperbola (Eq. (A.15))

$$v_0 = \frac{\frac{E_T\left(\, k_{+2} K'_m\, K'_i\, K_i + k_{+4}\left(K_m\, K'_i + K'_m K_i\right)[C]\right)}{K'_m\, K'_i\, K_i + \left(K_m\, K'_i + K'_m K_i\right)[C]}[A]}{\frac{K_m\, K'_m K'_i (K_i + [C])}{K'_m\, K_i K'_i + \left(K_m\, K'_i + K'_m K_i\right)[C]} + [A]} \qquad \text{(A.15, Eq.5 in the text)}$$

When reformulated in terms of total glucose concentration [G], Eq. (A.15) becomes:

$$v_0 = \frac{E_T\{k_{+2}\, K'_m K_i\, K'_i (R+1)[G] + k_{+4} R(K_m\, K'_i + K'_m K_i)[G]^2\}}{K_m\, K'_m K_i\, K'_i (R+1)^2 + K'_m\, K'_i (R+1)(K_m R + K_i)[G] + R(K_m\, K'_i + K'_m K_i)[G]^2}$$

(A.16, Eq.6 in the text)

Equation (A.16) predicts the dependence of the reaction rate of aldose reduction versus the total aldose concentration in the case of the mixed noncompetitive type of partial inhibition. Computer-aided simulations of double reciprocal plots of Eq. (A.16) end either with upward or downward curves depending on the imposed relative values of K_i and K'_i (see text, Fig. 5).

Section III- *Partial inhibition for an uncompetitive model of action of aldose hemiacetal on free aldehyde reduction.*

When the model of Fig. 4 C is analyzed considering *EAC* at equilibrium and *EA* in steady state conditions, the general rate equation for the transformation of *A:*

$$v_0 = \frac{d[P]}{dt} = k_{+2}[EA] + k_{+4}[EAC]$$

becomes:

$$v_0 = \frac{E_T\left(k_{+2} + k_{+4}\frac{[C]}{K'_i}\right)}{\frac{K_m}{[A]} + \frac{[C]}{K'_i} + 1} \qquad \text{(A.17)}$$

Equation (A.17) describes the dependence of the reaction rate of glucose reduction as a function of the aldose free aldehyde and aldose hemiacetal concentrations in the case of a partial uncompetitive type of inhibition. When one of these two terms is kept constant, v_0 versus the second one is described again by a rectangular hyperbola:

$$v_0 = \frac{\frac{E_T\left(k_{+2}K'_i + k_{+4}[C]\right)}{\left(K'_i + [C]\right)}[A]}{\frac{K_m K'_i}{K'_i + [C]} + [A]} \qquad \text{(A.18, Eq.7 in the text)}$$

Making use of Eqs.(A.11) and (A.12), Eq. (A.18) can be reformulated in order to express the reaction rate in terms of total glucose concentration:

$$v_0 = \frac{E_T\{k_{+2}K'_i(R+1)[G] + k_{+4}R[G]^2\}}{K_m K'_i (R+1)^2 + K'_i (R+1)[G] + R[G]^2} \quad \text{(A.19, Eq.8 in the text)}$$

This equation, similarly to what obtained for a partial nonclassical competitive inhibition model (Eq. (A.13)), predicts for the partial uncompetitive inhibition an apparent cooperative dependence of the reaction rate on the total glucose concentration. However, in this case, the biphasic curves in the double reciprocal plots would appear with an upward curvature as occurs for apparent positive cooperativity or substrate inhibition models. This would not fit with the downward curves observed for long chain aldoses (see text, Figs. 1 and 3).

Section IV*-In defining the model of partial inhibition for aldose hemiacetal on free aldehyde reduction.*

By exploiting the hyperbolic behavior displayed by nonclassical competitive, mixed and uncompetitive types of partial inhibition (Eqs. (A.10), (A.15) and (A.18), respectively), when reaction rates as a function of the substrate concentration (i.e. free aldehyde form of the aldose) are measured at different fixed concentrations of the inhibitor, an array of straight lines for all models will be generated in double reciprocal plots. The secondary plots of intercepts with the ordinate axis ($Vmax^{app}$) and with the abscissa axis (K_M^{app}) versus the aldose hemiacetal concentration related to different kinetic models are described as follows:

a) For the nonclassical competitive partial inhibition (*nc*)

$$(nc)Vmax^{app} = E_T\left(\frac{k_{+2}\,K'_mK_i+k_{+4}K_m[C]}{K'_mK_i+K_m[C]}\right) \quad \text{(A.20)}$$

$$(nc)K_M^{app} = \frac{K_m\,K'_mK_i+K_m\,K'_m[C]}{K'_mK_i+K_m[C]} \quad \text{(A.21)}$$

b) For the uncompetitive partial inhibition (*uc*)

$$(uc)V_{max}^{app} = E_T\left(\frac{k_{+2}K_i+k_{+4}[C]}{K_i+[C]}\right) \quad \text{(A.22)}$$

$$(uc)K_M^{app} = \frac{K_m\,K'_i}{K'_i+[C]} \quad \text{(A.23)}$$

c) For the mixed noncompetitive partial inhibition (*mix*)

$$(mix)V_{max}^{app} = E_T\left(\frac{E_T\{k_{+2}\,K'_mK_i\,K'_i+k_{+4}(K_m\,K'_i+K'_mK_i)[C]}{K'_m\,K_i\;K'_i+(K_m\,K'_i+K'_mK_i)[C]}\right) \quad \text{(A.24)}$$

$$(mix)K_M^{app} = \frac{K_m\,K'_m\,K_i\;K'_i(1+[C])}{K'_m\,K_i\;K'_i+(K_m\,K'_i+K'_mK_i)[C]} \quad \text{(A.25)}$$

Section V*-The action of hemiacetal acting as competitive substrate of the free aldehyde for AR is described by a hyperbola.*

In the search for models able to fit the apparent cooperative behavior displayed by AR in reducing glucose, the possibility that glucose hemiacetal can bind the enzyme and undergo reduction competing with the free aldehyde form was considered (Fig. A.1).

This model of two antagonist competitive substrates for the same enzyme was previously shown to be described by a hyperbolic kinetic equation with respect to each substrate (44). In the present case, in which both substrates are transformed into the same product, the equation predicting the effect exerted on the reaction rate by the concentration of both the hemiacetal ring and the sugar free aldehyde can be formulated (Eq. (A.26)):

$$v_0 = \frac{E_T\left(k_{+2}K_M^C[A]+k_{+4}K_M^A[C]\right)}{K_M^A K_M^C+K_M^A[C]+K_M^C[A]} \qquad \text{(A.26)}$$

in which K_M^A and K_M^C represent the Michaelis constants of AR for the free aldehyde and hemiacetal, respectively. As shown, when one of these two supposed substrates is kept constant, the dependence of the reaction rate on the remaining one is hyperbolic. No assumptions were made concerning the reaction pathway of reduction of the hemiacetal. However, in any case, an in situ opening step of the hemiacetal ring on the enzyme, which may end up as *EA*, must be presumed. The only restriction imposed on the scheme is the occurrence of a fast return of *E'* to *E*, a restraint which would conceivably force the system to be described by a hyperbolic function. However, conditions with the potential to induce non-equilibrium measurements, such as a slow equilibration between *E'* and *E*, which may generate apparent cooperative behavior, would be buffered in the case of aldoses in which both free aldehyde and the supposed hemiacetal substrate are in equilibrium and simultaneously change at a constant ratio. Thus, in order to express the reaction rate in terms of total glucose concentration $[G]$, using Eqs.(A.11) and (A.12), Eq. (A.26) can be reformulated and expressed in the usual form of a rectangular hyperbola (Eq. (A.27)):

$$v_0 = \frac{\frac{E_T\left(k_{+2}K_M^C+k_{+4}K_M^A R\right)}{K_M^A R+K_M^C}[G]}{\frac{K_M^A K_M^C(R+1)}{K_M^A R+K_M^C}+[G]} \qquad \text{(A.27)}$$

This result does not appear to support the hypotheses of the participation of the hemiacetal form as an alternative substrate to the aldose free aldehyde in generating the apparent cooperative behavior displayed by AR in reducing aldoses.

Acknowledgements

This work was supported in part by Regione Toscana, Progetto IDARA and in part by Pisa University. We are indebted to Dr. G. Pasqualetti and Dr. R. Di Sacco (veterinary staff of Consorzio Macelli S. Miniato, Pisa) for their valuable co-operation in collecting the bovine lenses.

REFERENCES

1. Alexiou, P., Pegklidou, K., Chatzopoulou, M., Nicolaou, I., and Demopoulos, V.J. (2009) Aldose reductase enzyme and its implication to major health problems of the 21$^{(st)}$ century. *Curr. Med. Chem.***16**,734-752.

2. Del Corso, A., Cappiello, M., and Mura, U. (2008) From a dull enzyme to something else: facts and perspectives regarding aldose reductase. *Curr. Med. Chem.* **15**, 1452-1461.

3. Kinoshita, J.H. (1974) Mechanisms initiating cataract formation. *Invest. Ophthalmol. Vis. Sci.* **13**, 713-724

4. Lee, A.Y., and Chung, S.S. (1999) Contributions of polyol pathway to oxidative stress in diabetic cataract. *FASEB J.* **13**, 23-30.

5. Hamada, Y., Araki, N., Koh, N, Nakamura, J., Horiuchi, S., and Hotta, N. (1996) Rapid formation of advanced glycation end products by intermediate metabolites of glycolytic pathway and polyol pathway. *Biochem. Biophys. Res. Commun.* **228**, 539-543.

6. Vander Jagt, D.L., Kolb, N.S., Vander Jagt, T.J., Chino, J., Martinez, F.J., Hunsaker, L.A., and Royer R.E. (1995) Substrate specificity of human aldose reductase: identification of 4-hydroxynonenal as an endogenous substrate. *Biochim. Biophys. Acta* **1249**, 117-126.

7. Srivastava, S., Chandra, A., Bhatnagar, A., Srivastava, S.K., and Ansari, N.H. (1995) Lipid peroxidation product, 4-hydroxynonenal and its conjugate with GSH are excellent substrates of bovine lens aldose reductase. *Biochem. Biophys. Res. Commun.* **217**, 741-746.

8. Rittner, H.L., Hafner, V., Klimiuk, P.A., Szweda, L.I., Goronzy, J.J., and Weyand, C.M. (1999) Aldose reductase functions as a detoxification system for lipid peroxidation products in vasculitis. *J. Clin. Invest.* **103**, 1007-1013.

9. Nishinaka, T., and Yabe-Nishimura, C. (2001) EGF receptor-ERK pathway is the major signaling pathway that mediates upregulation of aldose reductase expression under oxidative stress. *Free Radic. Biol. Med*. **31**, 205-216.

10. Seo, H.G., Nishinaka, T., and Yabe-Nishimura, C. (2000) Nitric oxide up-regulates aldose reductase expression in rat vascular smooth muscle cells: a potential role for aldose reductase in vascular remodeling. *Mol. Pharmacol.* **57**, 709-717.

11. Chatzopoulou, M., Pegklidou, K., Papastavrou, N., and Demopoulos, V.J. (2013) Development of aldose reductase inhibitors for the treatment of inflammatory disorders. *Expert Opin. Drug Discov.* **8**, 1365-1380.

12. Tammali, R., Ramana, K.V., Singhal, S.S., Awasthi, S., and Srivastava, S.K. (2006) Aldose reductase regulates growth factor-induced cyclooxygenase-2 expression and prostaglandin E2 production in human colon cancer cells. *Cancer Res.* **66**, 9705-9713.

13. Ramana, K.V., Bhatnagar, A., Srivastava, S., Yadav, U.C., Awasthi, S., Awasthi, Y.C., and Srivastava, S.K. (2006) Mitogenic responses of vascular smooth muscle cells to lipid peroxidation-derived aldehyde 4-hydroxy-trans-2-nonenal (HNE): role of aldose reductase-catalyzed reduction of the HNE-glutathione conjugates in regulating cell growth. *J. Biol. Chem.* **281**, 17652-17660.

14. Chang, K.C., Ponder, J., Labarbera, D.V., and Petrash, J.M. (2014) Aldose reductase inhibition prevents endotoxin-induced inflammatory responses in retinal microglia. *Invest. Ophthalmol. Vis. Sci.* **55**, 2853-2861.

15. Del-Corso, A., Balestri, F., Di Bugno, E., Moschini, R., Cappiello, M., Sartini, S., La-Motta, C., Da-Settimo, F., and Mura, U. (2013) A new approach to control the enigmatic activity of aldose reductase. *PLoS ONE* 10.1371/journal.pone.0074076.

16. Grimshaw, C.E., Shahbaz, M., Jahangiri, G., Putney, C.G., McKercher, S.R. and Mathur, E.J. (1989) Kinetic and structural effects of activation of bovine kidney aldose reductase. *Biochemistry* **28**, 5343-5353.

17. Sheaff, C.M., and Doughty, C.C. (1976) Physical and kinetic properties of homogenous bovine lens aldose reductase. *J. Biol. Chem*. **251**, 2696-2702.

18. Daly, A.K., and Mantle, T.J. (1982) Purification and characterization of the multiple forms of aldehyde reductase in ox kidney. *Biochem. J.* **205**, 373-380.

19. Conrad, S.M., and Doughty, C.C. (1982) Comparative studies on aldose reductase from bovine, rat and human lens. *Biochim. Biophys. Acta* **708**, 348-357.

20. Halder, A.B., and Crabbe, M.J. (1984) Bovine lens aldehyde reductase (aldose reductase). Purification, kinetics and mechanism. *Biochem. J.* **219**, 33-39.

21. Grimshaw, C.E., and Lai, C.J. (1996) Oxidized aldose reductase: in vivo factor not in vitro artifact. *Arch. Biochem. Biophys.* **327**, 89-97.

22. Poulsom, R. (1986) Inhibition of hexonate dehydrogenase and aldose reductase from bovine retina by sorbinil, statil, M79175 and valproate. *Biochem. Pharmacol*. **35**, 2955-2959.

23. Dons, R.F., and Doughty, C.C. (1976) Isolation and characterization of aldose reductase from calf brain. *Biochim. Biophys. Acta* **452**, 1-12.

24. Håstein, T., and Velle, W. (1969) Purification and properties of aldose reductase from the placenta and the seminal vescicle of the sheep. *Biochim. Biophys. Acta* **178**, 1-10.

25. Del Corso, A., Barsacchi, D., Giannessi, M., Tozzi, M.G., Camici, M., and Mura, U. (1989) Change in stereospecificity of bovine lens aldose reductase modified by oxidative stress. *J. Biol. Chem.* **264**, 17653-17655.

26. Srivastava, S.K., Hair, G.A., and Das, B. (1985) Activated and unactivated forms of human erythrocyte aldose reductase. *Proc. Natl. Acad. Sci. USA* **82**, 7222-7226.

27. Grimshaw, C.E., Shahbaz, M., and Putney, C.G. (1990) Mechanistic basis for nonlinear kinetics of aldehyde reduction catalyzed by aldose reductase. *Biochemistry* **29**, 9947-9945.

28. Morjana, N.A., Lyons, C., and Flynn, T.G. (1989) Aldose reductase from human psoas muscle: affinity labeling of an active site lysine by pyridoxal 5'- phosphate and pyridoxal 5'- diphospho-5-adenosine. *J. Biol. Chem.* **264**, 2912-2919.

29. Giannessi, M., Del Corso, A., Cappiello, M., Voltarelli, M., Marini, I., Barsacchi, D., Garland, D., Camici, M., and Mura, U. (1993) Thiol-dependent metal-catalyzed oxidation of bovine lens aldose reductase. I. Studies on the modification process. *Arch. Biochem. Biophys.* **300**, 423-429.

30. Cappiello, M., Voltarelli, M., Giannessi, M., Cecconi, I., Camici, G., Manao, G., Del Corso, A. and Mura, U. (1994) Glutathione dependent modification of bovine lens aldose reductase. *Exp. Eye Res.* **58**, 491-501.

31. Bohren, K.M., and Gabbay, K.H. (1993) Cys298 is responsible for reversible thiol-induced variation in aldose reductase activity. *Adv. Exp. Med. Biol.* **328**, 267-277.

32. Bhatnagar, A., Liu, S.Q., Petrash, J.M., and Srivastava, S.K. (1992) Mechanism of inhibition of aldose reductase by menadione (vitamin K3). *Mol. Pharmacol.* **42**, 917-921.

33. Vilardo, P.G., Scaloni, A., Amodeo, P., Barsotti, C., Cecconi, I., Cappiello, M., Lopez Mendez, B., Rullo, R., Dal Monte, M., Del Corso, A., and Mura, U. (2001) Thiol/disulfide interconversion in bovine lens aldose reductase induced by intermediates of glutathione turnover. *Biochemistry* 40, 11985-11994.

34. Cappiello, M., Voltarelli, M., Cecconi, I., Vilardo, P.G., Dal Monte, M., Marini, I., Del Corso, A., Wilson, D.K., Quiocho, F.A., Petrash, J.M., and Mura, U. (1996) Specifically targeted modification of human aldose reductase by physiological disulfides. *J. Biol. Chem.* **271**, 33539-33544.

35. Cappiello, M., Vilardo, P.G., Cecconi, I., Leverenz, V., Giblin, F.J., Del Corso, A., and Mura, U. (1995) Occurrence of glutathione-modified aldose reductase in oxidatively stressed bovine lens. *Biochem. Biophys. Res. Commun.* **207**, 775-782.

36. Cappiello, M., Vilardo, P.G., Micheli, V., Jacomelli, G., Banditelli, S., Leverenz, V., Giblin, F.J., Del Corso, A., and Mura, U. (2000) Thiol disulfide exchange modulates the activity of aldose reductase in intact bovine lens as a response to oxidative stress. *Exp. Eye Res.* **70**, 795-803.

37. Moschini, R., Peroni, E., Rotondo, R., Renzone, G., Melck, D., Cappiello, M., Srebot, M., Napolitano, E., Motta, A., Scaloni, A., Mura, U., and Del Corso, A. (2015) $NADP^+$-dependent dehydrogenase activity of carbonyl reductase on glutathionyl-hydroxynonanal as a new pathway for hydroxynonenal detoxification. *Free Radic. Biol. Med*. **83**, 66-76.

38. Balestri, F., Cappiello, M., Moschini, R., Rotondo, R., Buggiani, I., Pelosi, P., Mura, U., and Del Corso, A. (2015) L-Idose: an attractive substrate alternative to D-glucose for measuring aldose reductase activity. *Biochem. Biophys. Res. Commun*. **456**, 891-895.

39. Del Corso, A., Barsacchi, D., Giannessi, M., Tozzi, M.G., Camici, M., Houben, J.L., Zandomeneghi, M., and Mura, U. (1990) Bovine lens aldose reductase: tight binding of the pyridine coenzyme. *Arch. Biochem. Biophys.* **283**, 512-518.

40. Laemmli, U.K. (1970) Cleavage of structural proteins during the assembly of the head of bacteriophage T4. *Nature* **227**, 680-685.

41. Wray, W., Boulikas, T., Wray, V.P., and Hancock, R. (1981) Silver staining of proteins in polyacrylamide gels. *Anal. Biochem.* **118**, 197-203.

42. Bradford, M.M. (1976) A rapid and sensitive method for the quantitation of microgram quantities of protein utilizing the principle of protein-dye binding. *Anal. Biochem.* **72**, 248-254.

43. Dworkin, J.P. and Miller, S.L. (2000) A kinetic estimate of the free aldehyde content of aldoses. *Carbohydr. Res.* **329**, 359-363.

44. Cornish-Bowden, A. (2012) *Fundamentals of Enzyme Kinetics,* 4th Ed., Wiley-VCH Verlag Gmbh & Co. KGaA, Weinheim, Germany.

45. Inagaki, K., Miwa, I., and Okuda, J. (1982) Affinity purification and glucose specificity of aldose reductase from bovine lens. *Arch. Biochem. Biophys.* **216**, 337-344.

46. Grimshaw, C.E. (1986) Direct measurement of the rate of ring opening of D-glucose by enzyme catalyzed reduction. *Carbohyd. Res.* **148**, 345-358]

47. Segel, I.H. (1993) *Enzyme Kinetics,* John Wiley & Sons.

48. Morjana, N.A., and Flynn, T.G. (1989) Aldose reductase from human psoas muscle: purification, substrate specificity, immunological characterization and effect of drugs and inhibitors. *J. Biol. Chem.* **264**, 2906-2911.

49. Del Corso, A., Dal Monte, M., Vilardo, P.G., Cecconi, I., Moschini, R., Banditelli, S., Cappiello, M., Tsai, L., and Mura, U. (1998) Site-specific inactivation of aldose reductase by 4-hydroxynonenal. *Arch. Biochem. Biophys.* **350**, 245-248.

50. Hayman, S. and Kinoshita, J.H. (1965) Isolation and properties of lens aldose reductase. *J. Biol. Chem.* **240**, 77-882.

51. Petrash, J.M., Harter, T.M., Devine, C.S., Olins, P.O., Bhatnagar, A., Liu, S.Q., and Srivastava, S.K. (1992) Involvement of cysteine residues in catalysis and inhibition of human aldose reductase. Site-directed mutagenesis of Cys-80, -298, and -303. *J. Biol. Chem.* **267**, 24833-24840.

52. Bhatnagar, A., Liu, S.Q., Ueno, N., Chakrabarti, B., and Srivastava S.K. (1994) Human placental aldose reductase: role of Cys-298 in substrate and inhibitor binding. *Biochim. Biophys. Acta* **1205**, 207-214.

53. Gabbay, K.H., and Tze, W.J. (1972) Inhibition of glucose-induced release of insulin by aldose reductase inhibitors. *Proc. Natl. Acad. Sci. USA* **69**, 1435-1439.

54. Vander Jagt, D.L., Hunsaker, L.A., Robinson, B., Stangebye, L.A., and Deck, L.M. (1990) Aldehyde and aldose reductases from human placenta. Heterogeneous expression of multiple enzyme forms. *J. Biol. Chem.* **265**, 10912-10918.

55. Costantino, L., Rastelli, G., Vescovini, K., Cignarella, G., Vianello, P., Del Corso, A., Cappiello, M., Mura, U., and Barlocco, D. (1996) Synthesis, activity, and molecular modeling of a new series of tricyclic pyridazinones as selective aldose reductase inhibitors. *J. Med.Chem*. **39**, 4396-4405.

56. Kumar, H., Shah, A and Sobhia, M.E. (2012) Novel insights into the structural requirements for the design of selective and specific aldose reductase inhibitors. *J. Mol. Model.* **18**, 1791-1799.

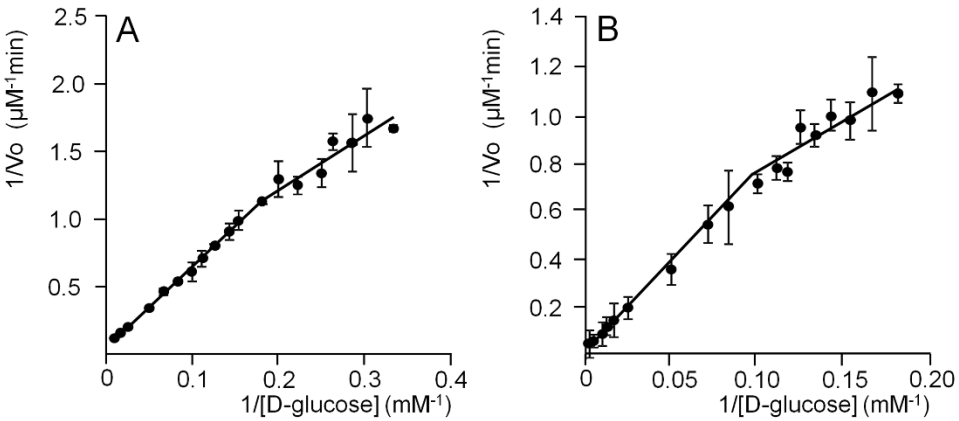

FIGURE 1. The reduction of D-glucose catalyzed by aldose reductase. The initial rate measurements of the reduction of D-glucose in the presence of either *b*AR at a final concentration of 11 mU mL^{-1} (*Panel A*), or *h*AR at a final concentration of 53 mU mL^{-1} (*Panel B*), are reported in double reciprocal plots. Straight lines interpolating experimental data were drawn on the basis of the kinetic parameters evaluated by nonlinear regression analysis. Error bars (when not visible are

within the symbol size) represent the standard deviations of the mean, from at least three independent measurements.

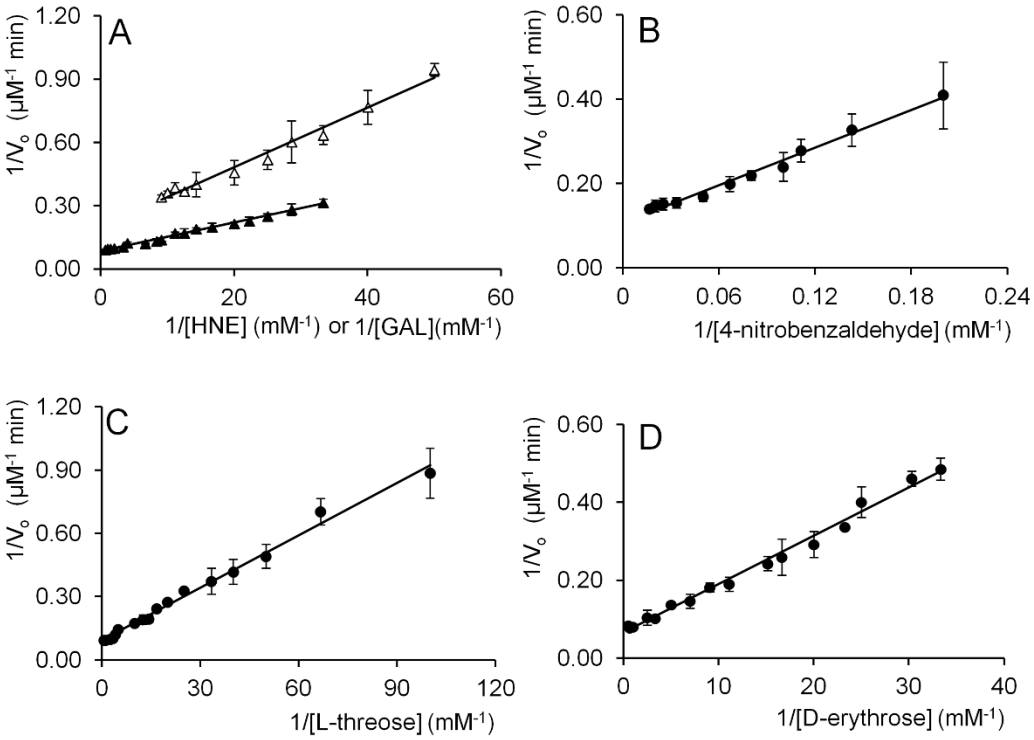

FIGURE 2. Double reciprocal plots for the reduction of different aldehydes catalyzed by aldose reductase. The initial rate measurements of the reduction of different AR substrates are reported as double reciprocal plots. *Panel A*: GAL (open triangles), HNE (closed triangles); *Panels B*, *C* and *D* refer to 4-nitrobenzaldehyde, L-threose and D-erythrose, respectively. The assays were performed in the presence of *h*AR at a final concentration of 7 mU mL^{-1} for GAL, HNE and 4-nitrobenzaldehyde and 14 mU mL^{-1} for threose and erythrose. Error bars (when not visible are within the symbol size) represent the standard deviations of the mean from at least three independent measurements. Straight lines interpolating experimental data were drawn on the basis of the kinetic parameters evaluated by nonlinear regression analysis.

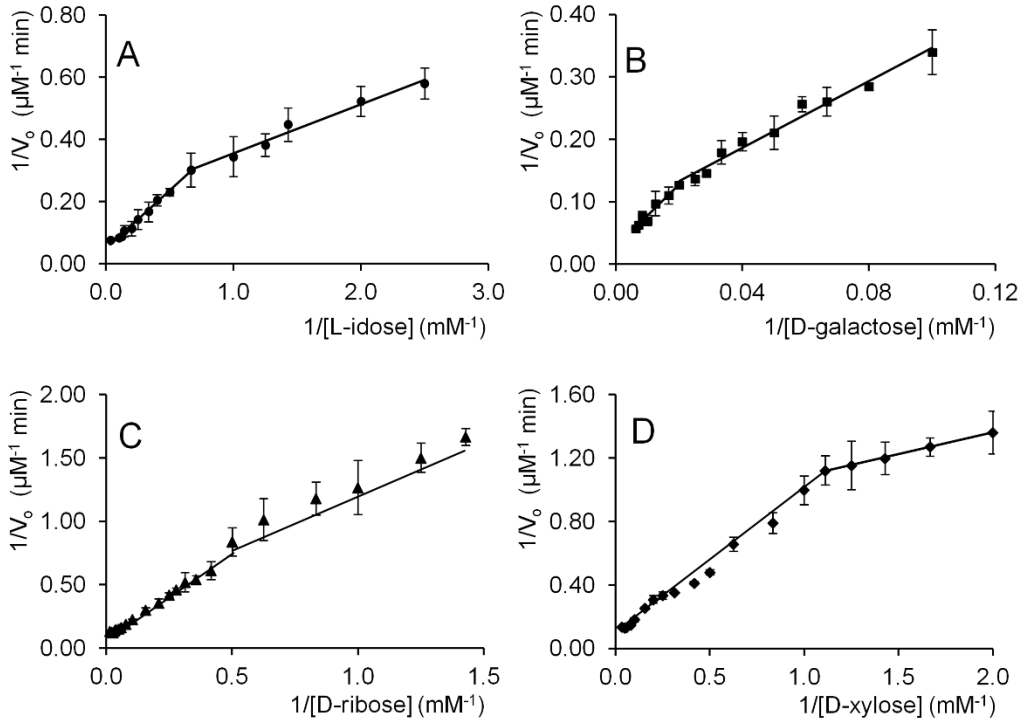

FIGURE 3. Double reciprocal plots for the reduction of different aldoses catalyzed by aldose reductase. The initial rate measurements of the reduction of L-idose (*Panel A*), D-galactose (*Panel B*), D-ribose (*Panel C*) and D-xylose (*Panel D*) are reported as double reciprocal plots. The assays were performed in the presence of *h*AR at a final concentration of 16 mU mL^{-1} for L-idose, 14 mU mL^{-1} for D-ribose and D-xylose and 36 mU mL^{-1} for D-galactose. Error bars (when not visible are within the symbols size) represent the standard deviations of the mean from at least three independent measurements. Straight lines were drawn at high and low concentration ranges of different aldoses on the basis of the kinetic parameters evaluated by nonlinear regression analysis. Highest values of the low concentration ranges are. 0.9, 1.5, 2 and 50 mM for D-xylose, L-idose, D-ribose and D-galactose, respectively.

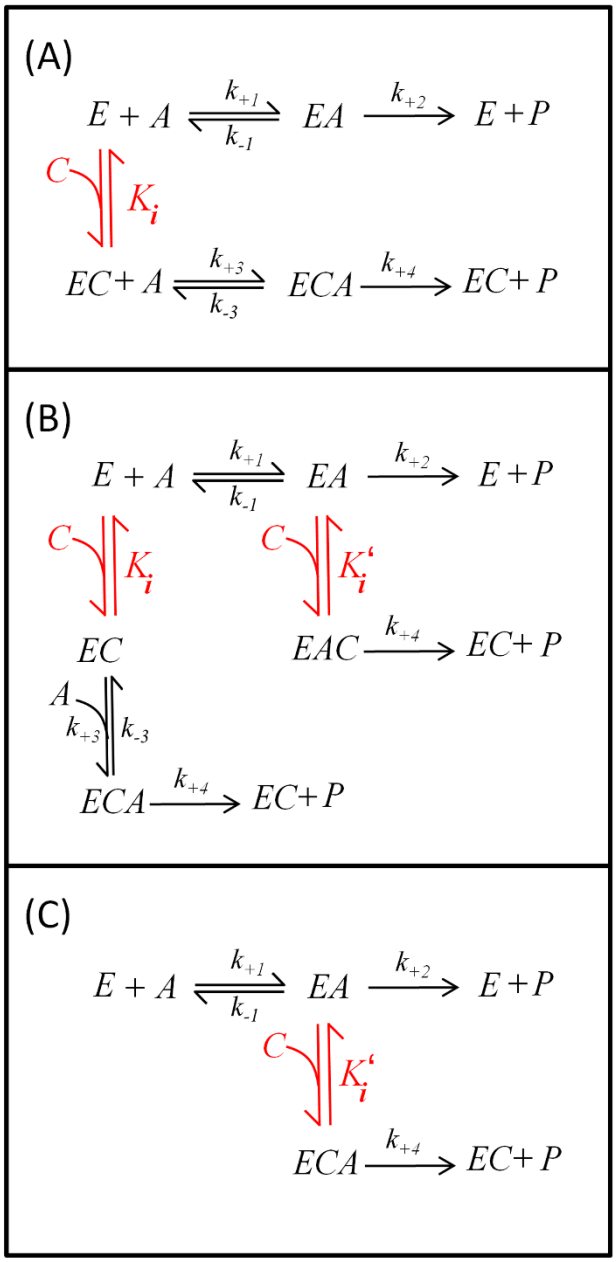

FIGURE 4. Kinetic models for aldose reduction by AR. The symbols *A* and *C* represent the aldose free aldehyde and the hemiacetal form, respectively. *EA* and *EC* represent the binary complexes of AR with *A* and *C*, respectively, while *ECA* and *EAC* represent the ternary complexes which derive from the two indicated interaction pathways. Lower case "*k*" refer to kinetic constants; upper case "*K*" refer to dissociation equilibrium constants. *Panel A*: model of partial nonclassical competitive inhibition exerted by the hemiacetal on aldose reduction. *Panel B*: model of partial mixed noncompetitive inhibition. *Panel C:* model of partial uncompetitive inhibition.

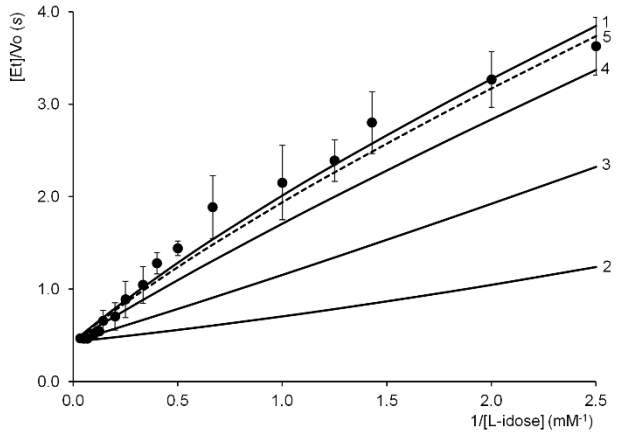

FIGURE 5. Simulation of the apparent negative cooperative behavior of AR acting on L-idose. Double reciprocal plots of reaction rates (v_0/E_T) versus L-idose concentration were generated by computer-assisted simulation either using Eq. 3, which describes the kinetic model of partial nonclassical competitive inhibition (curve 1), or using Eq. 6, which describes the kinetic model of partial mixed noncompetitive inhibition (curves 2 to 5). Curve 1 originates from Eq. 3 using the values of 1.0 µM and 3.4 µM for K_m and K'_m, respectively, and values of 1.24 s^{-1} and 2.32 s^{-1} for k_{+2} and for k_{+4}, respectively, as derived from the present study and by imposing a K_i of 2.5 x 10^{-4} M. Curves 2, 3, 4 and 5 were generated from Eq. 6 using the above parameters and a K'_i/Ki ratio of 0.5, 2, 10 and 50, respectively.

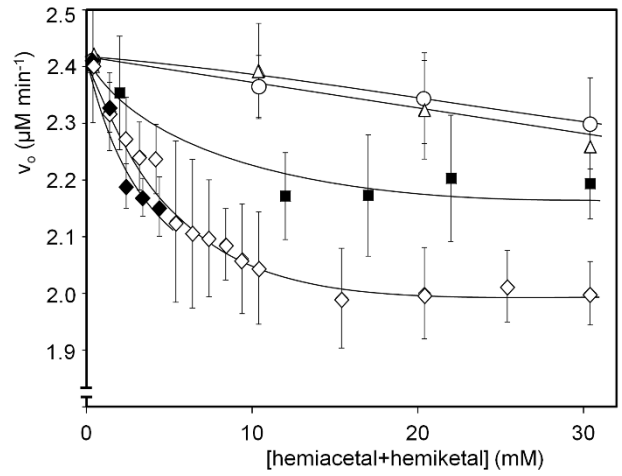

FIGURE 6. Effect of different hemiacetals/hemiketals on aldose reduction. The reaction rate of L-idose reduction was measured using 0.4 mM of the aldose at the indicated concentrations of the following: D-glucose (closed diamonds), L-glucose (open diamonds), D-fructose (open triangles)

and D-sorbose (open circles). Closed squares refer to the reduction of 2 mM D-ribose in the presence of the indicated L-glucose concentration. The *h*AR present in the assay mixture accounted for 21 mU mL^{-1} and the reaction rate is expressed as a percentage of the value measured in the absence of effectors. The abscissa values represent the total concentration of hemiacetals plus hemiketals present in the assay mixtures.

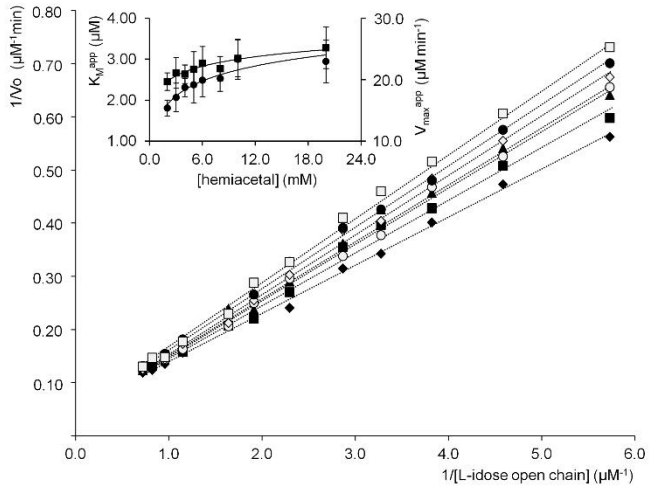

FIGURE 7. Kinetic analysis of the inhibition of L-idose reduction by aldose hemiacetal. Assay mixtures were assembled in order to measure the rate of the reduction of L-idose at different substrate concentrations and at different levels of L-glucose by keeping the total hemiacetal concentration (L-glucose hemiacetal plus L-idose hemiacetal) constant. The data, reported in a double reciprocal plot, refer to total hemiacetal concentrations ranging from 1 mM (closed diamonds) to 20 mM (open squares). Straight lines interpolating experimental data were drawn on the basis of the kinetic parameters evaluated by nonlinear regression analysis. In the *Inset*, the values of apparent K_M (circles) and apparent k_{cat} (squares) are reported in a secondary plot as a function of the total hemiacetal concentration. The limit values at zero and at the saturating hemiacetal concentration were determined through the analysis of the data by nonlinear fitting method with a confidence limit of 90% and a Pearson coefficient (R) of 0.999 (see Section 2.4). Assays were performed using 34 mU mL^{-1} of *h*AR.

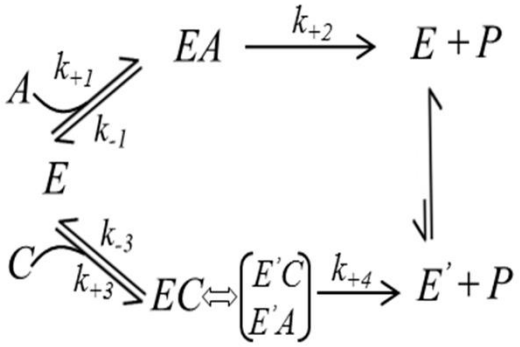

FIGURE A.1. Aldose reduction by AR through the participation of the hemiacetal (*C*) as substrate. *A* and *C* represent the aldehyde open chain of the aldose and the closed hemiacetal form, respectively. *EA* and *EC* represent the binary complexes of AR with *A* and *C*, respectively. *E'C* and *E'A* represent generic forms of the *EC* evolution bringing the complex toward product formation; *E'* represents the free enzyme form as it comes from the catalytic step. Lower case constants refer to kinetic constants.